

How bright are the gaps in circumbinary disk systems?

jms@astro.princeton.edu

Ji-Ming Shi¹ and Julian H. Krolik²

ABSTRACT

When a circumbinary disk surrounds a binary whose secondary’s mass is at least $\sim 10^{-2} \times$ the primary’s mass, a nearly empty cavity with radius a few times the binary separation is carved out of the disk. Narrow streams of material pass from the inner edge of the circumbinary disk into the domain of the binary itself, where they eventually join onto the small disks orbiting the members of the binary. Using data from 3-d MHD simulations of this process, we determine the luminosity of these streams; it is mostly due to weak laminar shocks, and is in general only a few percent of the luminosity of adjacent regions of either the circumbinary disk or the “mini-disks”. This luminosity therefore hardly affects the deficit in the thermal continuum predicted on the basis of a perfectly dark gap region.

Subject headings: accretion, accretion disks — binaries: general — MHD — methods: numerical

1. Introduction

Circumbinary disks are ubiquitous astronomical objects. They are often observed around young binary stars (e.g., Dutrey et al. 1994; Andrews & Williams 2005) and may have already been detected in disk-planet systems (Reggiani et al. 2014; Biller et al. 2014; Sallum et al. 2015). They may also be present around supermassive binary black holes (SMBBHs) as galaxies merge (Begelman et al. 1980; Ivanov et al. 1999; Merritt & Milosavljević 2005). When the mass ratio is not too far from unity, the binary clears out a low density gap in the disk center, crossed by one or two narrow streams. Emanating from the inner edge of the circumbinary disk, some of the matter in these streams reaches “mini-disks” attached to the members of the binary, while some of the matter suffers strong torques and swings back out to the circumbinary disk. (Artymowicz & Lubow 1994; Günther & Kley 2002; MacFadyen & Milosavljević 2008; Cuadra et al. 2009; Hanawa et al. 2010; de Val-Borro et al. 2011; Roedig et al. 2012; Shi et al.

2012; D’Orazio et al. 2013; Farris et al. 2014; Shi & Krolik 2015; D’Orazio et al. 2016).

A natural question to ask is therefore: does this distinctive region produce a characteristic light signal? There is some controversy about the answer to this question. A number of papers have argued that the gap region of a circum-SMBBH disk, including the streams, should be relatively dim, and would therefore produce a dip in the thermal disk spectrum over a specific range of wavelengths dependent upon the parameters of the system (Roedig & Sesana 2012; Tanaka et al. 2012; Gültekin & Miller 2012; Kocsis et al. 2012; Tanaka & Haiman 2013; Roedig et al. 2014). Others have pointed to events on either the inside or the outside of the gap as creating distinct radiative features. It has been suggested, for example, that because the accretion rate across the gap is in general modulated strongly at a frequency comparable to the orbital frequency, so, too, should the bolometric accretion luminosity from the mini-disks (MacFadyen & Milosavljević 2008; D’Orazio et al. 2013). However, this is unlikely to occur because most of the luminosity from the mini-disks is made in their inner radii, and the inflow time from the rim of a mini-disk is much longer than the binary orbital period (Farris et al. 2014). On

¹Department of Astrophysical Sciences, Princeton University, 4 Ivy Lane, Princeton, NJ 08544

²Department of Physics and Astronomy, Johns Hopkins University, Baltimore, MD 21218

the other hand, [Roedig et al. \(2014\)](#) pointed out that the shock created where streams from the circumbinary disk hit the outer rim of the mini-disks should be quite bright, radiating primarily in the hard X-ray band, and, unlike the accretion luminosity, its output should reflect the modulation because the local Compton cooling time is short. [Noble et al. \(2012\)](#) identified another possible signature in thermal emission from the inner edge of the circumbinary disk due to shocks driven by returning streams. The radially integrated luminosity of this component is consistent with the amount of work done by the binary torque on the disk, as argued in [Shi et al. \(2012\)](#). Recently, however, [Farris et al. \(2014\)](#) have computed thermal emission from the gap proper as well as its edges based on their 2D hydrodynamic simulations, reaching the surprising conclusion that, far from being dim, the streams can actually be more luminous than the inner region of the circumbinary disk.

Unfortunately, this last effort depended upon an assumption with potentially significant implications for the result. Their heating rate was calculated on the basis of a phenomenological “ α model” shear viscosity. This model was invented by [Shakura & Sunyaev \(1973\)](#) to mock up internal disk accretion stresses now known to be due to MHD turbulence driven by the magneto-rotational instability ([Balbus & Hawley 1998](#)). Because the dynamical state of the streams is quite different from the nearly-circular orbits inside an accretion disk, it is not at all clear whether this model is applicable to them.

In this paper we set out to test these assumptions by measuring the heating rate in the streams as determined by a pair of 3-d MHD simulations first reported in [Shi & Krolik \(2015\)](#). These simulations make no phenomenological assumptions relevant to dissipative processes, and should therefore provide an accurate measure of local heating whether due to small-scale turbulence or coherent dissipative features like shocks. Despite their assumed isothermal equation of state, we can also evaluate pdV temperature changes from their stored velocity data.

2. Methods

Our data are from the simulations of [Shi & Krolik \(2015\)](#). Two 3-d MHD simulations of cir-

cumbinary disks around circular orbiting binaries of mass ratio $q = 1$ and 0.1 are analyzed in this work. The simulations adopted a global isothermal equation of state. Shocks are captured with von Neumann-Richtmyer explicit bulk viscosity defined as ([Stone & Norman 1992](#))

$$\nu_{\text{sh}} \equiv \begin{cases} C_{\text{sh}} \Delta x^2 (-\nabla \cdot \mathbf{v}) & \text{if } \nabla \cdot \mathbf{v} < 0 \\ 0 & \text{otherwise,} \end{cases} \quad (1)$$

where Δx is the cell width, and $C_{\text{sh}} = 2$ is a fixed number characterizing the number of cells over which the artificial bulk viscosity spreads a shock. The corresponding dissipation rate can be integrated over the volume of the gap region via:

$$\begin{aligned} Q_{\text{sh}} &\equiv \int r dr d\phi dz [\rho \nu_{\text{sh}} (\nabla \cdot \mathbf{v})^2] \\ &= \int r dr d\phi \Sigma \langle \nu_{\text{sh}} (\nabla \cdot \mathbf{v})^2 \rangle_{\rho,z} \\ &= \int r dr d\phi q_{\text{sh}}. \end{aligned} \quad (2)$$

Here we define the rate of shock dissipation per unit surface area as

$$q_{\text{sh}} \equiv \Sigma \langle \nu_{\text{sh}} (\nabla \cdot \mathbf{v})^2 \rangle_{\rho,z}. \quad (3)$$

This vertically-integrated quantity is useful to study because the principal dynamics of the streams are in the equatorial plane.

Our isothermal equation of state implicitly assumes that work done by adiabatic compression is immediately radiated away. However, it is also equally true that an isothermal equation of state *injects* heat during adiabatic expansion. The net of these two effects (if positive) is the fairest estimate of the actual luminosity associated with thermal work. We can calculate its magnitude by evaluating the $-p\nabla \cdot \mathbf{v}$ term in the hydrodynamic energy equation.

3. Results

3.1. Dissipation rate

In [Figure 1](#), we show snapshots of the dissipation rate per unit surface area in the horizontal disk plane. The shock heating (q_{sh}) is mostly confined within the gas stream and, as we will show later, is strongest when binary torques acting on the stream push it outward.

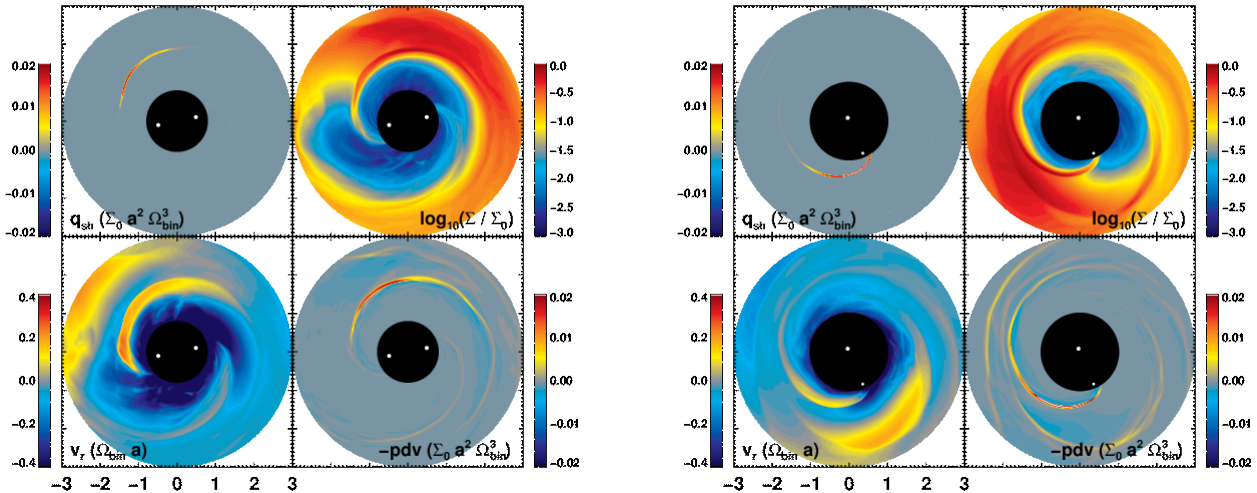


Fig. 1.— Snapshots of vertically-integrated shock dissipation rate per unit area (q_{sh}), surface density (Σ), density-weighted, vertically-averaged radial velocity (v_r), and vertically-integrated thermal work ($-pdV$) for equal mass (left four panels at $t = 1329\Omega_{\text{bin}}^{-1}$) and $q = 0.1$ case (right four panels, at $t = 1356\Omega_{\text{bin}}^{-1}$).

In Figure 2, we display the dissipation rate integrated out to r_{out} as a function of time. As can be seen, shocks are well-defined events, so we can easily choose an outer boundary for their contribution to the heating. By definition, the shock heating Q_{sh} is always positive. In the equal mass binary, the time averaged shock heating takes places mostly around $r \gtrsim 1.5a$, where the shocks are strongest. A smaller amount takes place at $r \sim 3a$ where the shocks propagate into the disk interior. On the other hand, in the $q = 0.1$ binary, the time averaged heating rate is distributed more broadly in radius over the range $a \lesssim r \lesssim 3a$.

In contrast, the $-pdV$ work is somewhat more broadly distributed spatially, and can have either sign. Although its absolute magnitude can be greater than that of q_{sh} , its variation in sign leads to substantial cancellation. In fact, Figure 2 shows that the net time-averaged $-pdV$ work is always negative, i.e., creates *cooling*, within the gap region. Indeed, it is particularly large and negative at the inner edge of the circumbinary disk, just inside the surface density maximum (see also Figure 4 of Shi & Krolik 2015). For our volume-integrated quantities, we therefore choose the gap’s outer edge $r_{\text{out}} = 2.5a$ for the equal mass

binary and $2.2a$ for the $q = 0.1$ case. We note that our qualitative conclusions, both about the net effect of adiabatic temperature changes and the overall magnitude of stream luminosity, do not depend in any significant way on the exact choice of r_{out} .

We plot the time history of the radially-integrated dissipation rates in Figure 3, normalizing the dissipation to the instantaneous value of $G\dot{M}/a$. The accretion rate is measured at the inner boundary r_{in} , and we neglect the small difference between $\dot{M}(r = r_{\text{in}})$ and $\dot{M}(r = a)$. We find: (1) Q_{sh} and $-pdV$ are comparable to one another, but in this volume-integrated sense $-pdV$ is a factor of a few smaller and generally negative. (2) both $q = 0.1$ and $q = 1$ show strong oscillations even after the normalization; the $q = 0.1$ case shows more regular and lower frequency fluctuations (when measured in units of Ω_{bin}^{-1}) although the amplitude is in general smaller than in the equal mass case. (3) in both cases and at all times, both heating rates are less than 10% of the total power that could be tapped from accretion; in an average sense, their magnitudes are closer to a few percent of that power. To be quantitative, the actual time-averaged normalized heating

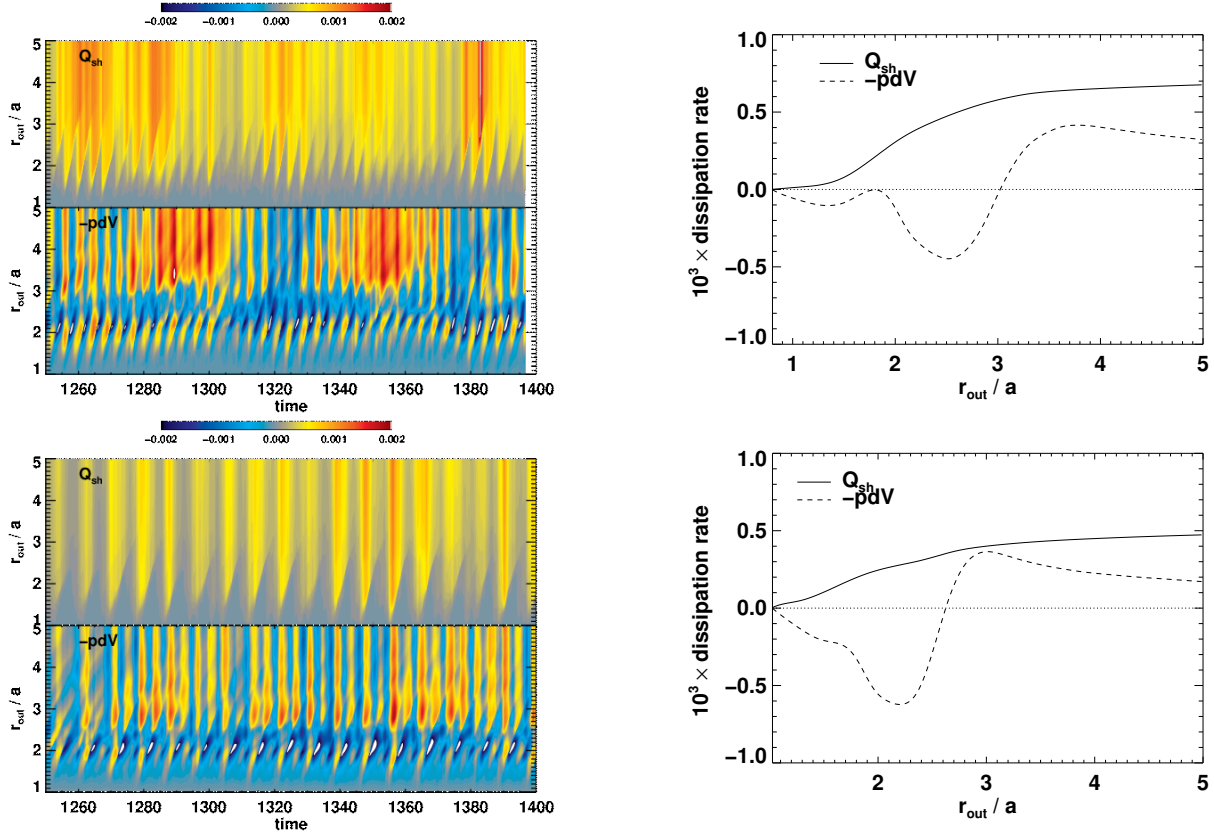


Fig. 2.— Integrated dissipation rates within radius r_{out} (in code units) as a function of r_{out} and time are shown in terms of space-time diagrams. Time-averaged values are shown on the right. Top two panels are for $q = 1$, bottom two for $q = 0.1$.

rates are: $\langle Q_{sh}/(GM\dot{M}/a) \rangle_t \simeq 0.037$ (0.017) for $q = 1$ ($q = 0.1$), $\langle -pdV/(GM\dot{M}/a) \rangle_t \simeq -0.031$ (-0.038) for $q = 1$ ($q = 0.1$).

Figure 4 shows the same evolution of dissipation but normalized with time averaged accretion $\langle GM\dot{M}/a \rangle_t$. Surprisingly, the amplitudes change rather little. The reason is that the heating rates are modulated at the same frequencies as the accretion rate, but with a phase offset. This offset provides an important clue to the mechanism driving the shocks.

To study this phase relationship, we compute the cross-correlation functions between the heating rates and the accretion rate. These are shown in Figure 5. When $q = 0.1$, there is a strong peak in the cross-correlation function indicating that fluctuations in the shock heating rate follow fluctuations in the accretion rate with a lag $\simeq 2\Omega_{bin}^{-1}$.

That mass-ratio also displays a weaker, but significant, peak at a slightly larger lag for fluctuations in the adiabatic compression work. Two peaks appear in the $q = 1$ case, but they are actually the same peak: both the accretion rate and the shock heating rate are modulated at a frequency $\simeq 1.5\Omega_{bin}$, whose period ($\sim 4\Omega_{bin}^{-1}$) is the separation between the two peaks. Thus, in this case, too, the heating rates follow variations in the accretion rate with a lag $\simeq 2\Omega_{bin}^{-1}$. This delay occurs because the shocks take place in matter that has fallen in almost to the inner cut-out, but then moves outward as binary torques raise its angular momentum. The outward acceleration takes $\simeq 2\Omega_{bin}^{-1}$ to be accomplished.

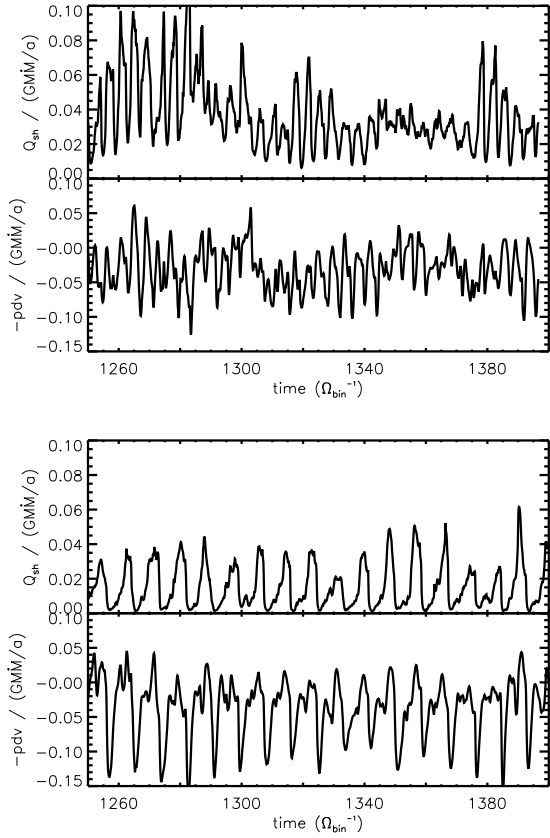


Fig. 3.— Time history of Q_{sh} and $-pdV$ normalized to the instantaneous GMM/a (at the inner boundary) for $q = 1$ (top two panels) and $q = 0.1$ (bottom two panels).

3.2. Gridscale dissipation

So far, we have identified sources of luminosity as either genuine shock heating or adiabatic compression. However, in turbulent fluids there can also be a contribution from subsonic dissipation acting on the scale of the smallest turbulent eddies, creating heat by dissipation of either fluid kinetic energy or magnetic fields. This kind of dissipation provides most of the heating in ordinary accretion disks; it is also the sort of heating that the α -model hopes to capture.

It is, however, very difficult to capture in a realistic way in fluid simulations because the physical dissipation lengthscale is very very small compared to feasible grid resolutions. Instead, numerical simulations mimic this dissipation by gridscale

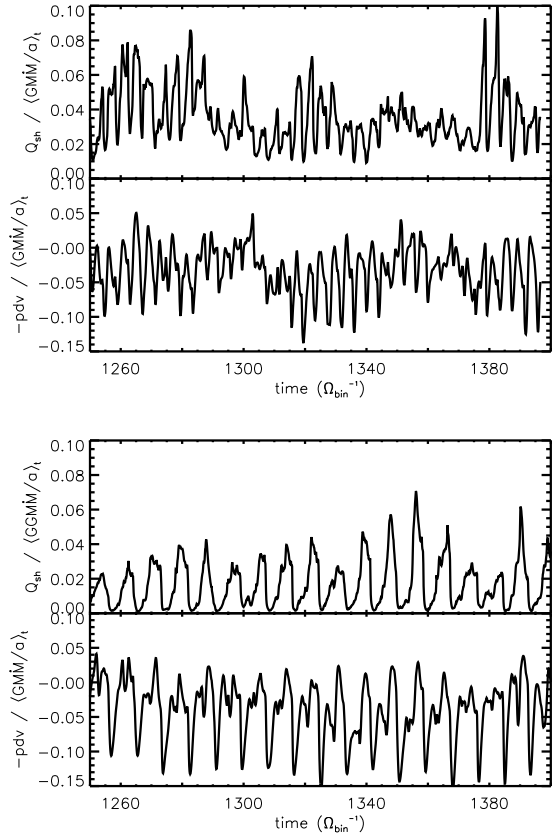


Fig. 4.— Same as Figure 3 but normalized to the time averaged $\langle GMM/a \rangle_t$ measured at the inner boundary.

numerical effects. Because MHD simulations can develop turbulence as a result of the magnetorotational instability, there is a reasonable hope that the turbulent cascade in such a simulation carries energy to the dissipation scale at the same rate as in a physical disk. Hydrodynamic disks do not exhibit turbulence; hence the insertion of phenomenological models to create dissipation. In energy-conserving (and non-isothermal) MHD simulations, the gridscale dissipation is automatically captured into heat. However, the ZEUS code used in these simulations solves an internal energy equation rather than a total energy equation, and our equation of state is isothermal. Nonetheless, it is still possible to estimate the magnitude of this sort of dissipation in our simulations by supposing that the shear part (the traceless part) of the velocity gradient tensor is comparable in magni-

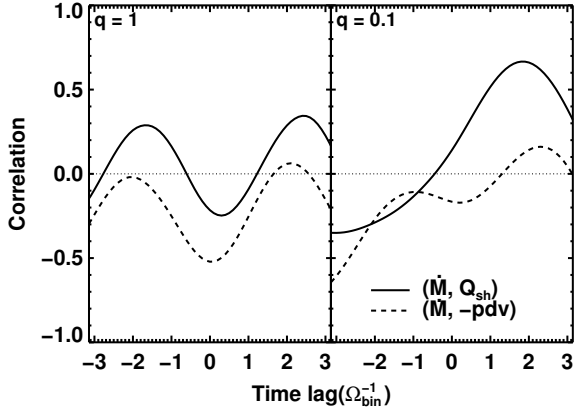


Fig. 5.— Cross correlation between the accretion rate and the dissipation rates. Shock heating variations follow accretion rate variations with a lag $\sim 2\Omega_{\text{bin}}^{-1}$. (black solid lines)

tude to the divergence part (the part containing non-zero trace), and then supposing that the numerical effective shear viscosity is comparable to the explicit artificial bulk viscosity.

In the bulk of the circumbinary disk, turbulent dissipation almost certainly dominates the local heating rate. However, the gap region is different. The streams are nearly laminar, i.e., their fluctuations in fluid quantities are small compared to their mean values. We quantify this statement by defining the fractional turbulent velocity amplitude as $\langle |v_z| \rangle_{\rho,z} / \langle (v_r^2 + \delta v_\phi^2 + v_z^2)^{1/2} \rangle_{\rho,z}$ and the fractional turbulent magnetic field amplitude as $\langle |B_z| \rangle_{\rho,z} / \langle \mathbf{B}^2 \rangle_{\rho,z}$. The values of these quantities are shown in Figure 6. The accretion streams' locations within these images are identified by the concentrated white contours, which show the surface density. Within the streams, the fractional turbulent amplitudes of both velocity and magnetic field are clearly much smaller than in the truly turbulent circumbinary disk: whereas both amplitudes are frequently $\simeq 0.5$ in the circumbinary disk, they are both almost always < 0.1 in the accretion streams, and frequently closer to 0.01. Because dissipation scales with the square of the fluctuation amplitude, we estimate that turbulent dissipation within the streams must be quite small compared to the shock heating, almost certainly $< 10^{-2}Q_{\text{shock}}$. In the streams, therefore, turbulent dissipation adds little heating to the already

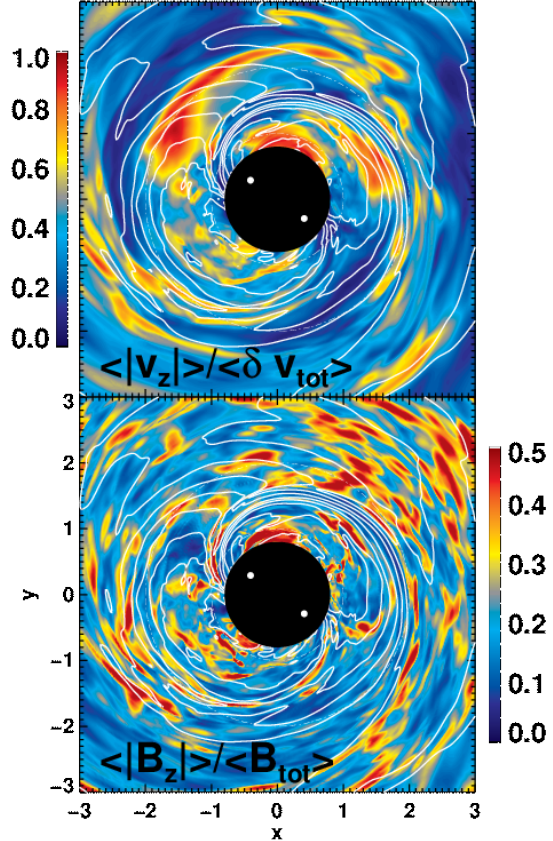


Fig. 6.— $\langle |v_z| \rangle_{\rho,z} / \langle (v_r^2 + \delta v_\phi^2 + v_z^2)^{1/2} \rangle_{\rho,z}$ (top) and $\langle |B_z| \rangle_{\rho,z} / \langle \mathbf{B}^2 \rangle_{\rho,z}$ (bottom) in color scales which characterize the amplitude of the turbulence. The overlaid surface density contours (in white) show ten consecutive values logarithmically scaled between 10^{-3} to 1. Clearly, within the gas stream (where contour lines concentrate) the turbulent amplitude is largely weaker than that in the disk body.

small amount created by shocks.

3.3. Thermal spectra

We now calculate the thermal spectrum of an accreting binary by taking account shock heating in the streams crossing the gap as well as accretion heating in both the circumbinary disk and the

mini-disks. For the two conventional disk regions, we follow [Roedig et al. \(2014\)](#). We define a characteristic temperature by assuming steady accretion and radiative cooling locally at $r = a$:

$$T_0 \equiv \left(\frac{3GM\dot{M}(a)}{8\pi\sigma a^3} \right)^{1/4}, \quad (4)$$

where $\dot{M}(a)$ is the time averaged accretion rate at $r = a$.¹ The effective temperature at any radius within either the circumbinary disk or the mini-disks would scale as

$$T_{\text{eff}}^{(\text{disk})}(r)/T_0 = \left(\frac{\dot{M}(r)}{\dot{M}(a)} \right)^{1/4} \left(\frac{a}{r} \right)^{3/4}, \quad (5)$$

where r is the distance from the system center-of-mass in the circumbinary disk, while it is the distance from the corresponding black hole in a mini-disk. The accretion rate is likewise divided into individual mini-disk portions. Our simulation achieved steady accretion out to $r \lesssim 4a$, so the local effective temperature in the circumbinary disk is mostly determined by the power law $r^{-3/4}$. We further assume the two mini-disks are filled to their tidal truncation radii. The temperature at the outside edges of individual mini-disks are calculated with equations (4-5) in [Roedig et al. \(2014\)](#), which assume the two mini-disks receive fractions $f_{1,2}$ of the total accretion rate, where $f_1 + f_2 = 1$ and $f_1/f_2 = q$.

Following [Roedig et al. \(2014\)](#), we write the spectral emissivity of all the disks, circumbinary or mini, in the form

$$L_{\epsilon}^{(\text{disk})} = \frac{32\pi a^2}{3h^3 c^2 g^4} (kT_0)^{8/3} \epsilon^{1/3} \int_{u_l}^{u_h} du \frac{u^{5/3}}{e^{u/g} - 1}, \quad (6)$$

where $\epsilon \equiv h\nu$, $u \equiv \epsilon/(kT_{\text{eff}}^{(\text{disk})})$, $g \simeq 1.7$ is the hardening factor due to strong electron scattering, and u_l and u_h are the lower and upper bounds of the integral, which are set by the effective temperatures at the inner and outer edge of the disk. The inner disks are integrated from $u_l = 0$ up to u_1 and u_2 defined in Equation (9-10) of [Roedig et al. \(2014\)](#); the emission of the outer disk is integrated from $r = r_{\text{out}}$ ($2.5a$ for the $q = 1$ binary and $2.2a$ for the $q = 0.1$ binary) out to $4a$.

¹For the $q = 0.1$ case, we neglect the small difference between $r = a$ and the inner simulational boundary, which is at $r \simeq 1.02$.

Similarly, the effective temperature of the stream shock regions can be scaled as

$$T_{\text{eff}}^{(\text{sh})}/T_0 = \left(\frac{8\pi a^3 q_{\text{sh}}}{3GM\dot{M}(a)} \right)^{1/4}. \quad (7)$$

As [Figure 1](#) illustrates, $T_{\text{eff}}^{(\text{sh})}$ is a strong function of position within the gap region. We can then integrate over the shock heating regions and find

$$L_{\epsilon}^{(\text{sh})} = \frac{8\pi a^2}{h^3 c^2 g^4} \epsilon^3 \int_{r_{\text{in}}}^{r_{\text{out}}} \frac{r/a}{e^{u/g} - 1} d\left(\frac{r}{a}\right) \frac{d\phi}{2\pi}, \quad (8)$$

where $u = \epsilon/(kT_{\text{eff}}^{(\text{sh})})$. Here $r_{\text{in}} = a$ and $r_{\text{out}} = 2.5a$ ($2.2a$) for the $q = 1$ ($q = 0.1$) case, as discussed in [section 3.1](#).

The resulting spectra are displayed in [Figure 7](#) for both mass-ratio cases. Clearly, the deep depression of the binary spectrum (black curve) is still present even after the radiation within the gap region (red dashed) is added. Compared to the radiation from the gap region that would have been emitted from a classic disk (no gap; blue dotted), the stream luminosity is two orders of magnitude smaller in amplitude, and what little is radiated is shifted to photons roughly a factor of two higher in energy. The time variation of the stream contribution to the spectrum is bounded by the two red dotted lines, which show the most extreme values of the luminosity found during our simulation. Even these extrema differ by only a factor of a few from the mean values, so at no time do they make significant contributions to filling the “notch” shown in the spectra of [Roedig et al. \(2014\)](#).

These results differ from those of [Farris et al. \(2015\)](#), who found, using the α -model, that emission from the streams can mask the “notches” completely. It appears that the α -model, designed to mimic turbulent dissipation through a “viscous” stress proportional to the local shear, overestimates the heating rate because there is substantial shear in the streams, but only weak turbulence. The actual stream luminosity is mainly due to laminar shocks, and is much smaller than the α -model estimate.

4. Conclusions and Implications

Given that shock heating in the streams is at most a few percent of the accretion luminosity

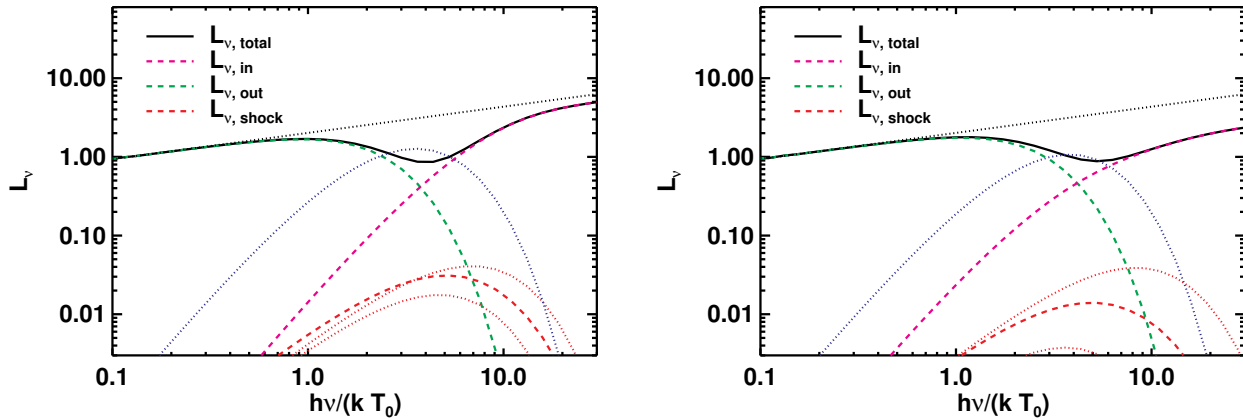


Fig. 7.— Thermal spectra for circumbinary disks with equal (left, $q = 1$) and unequal (right, $q = 0.1$) mass binaries. The solid black lines show the total spectra, while different components are in color as labeled in the legend. The red dashed curves show the time averaged values of the stream; the red dotted curves are the largest and smallest instantaneous contributions to the luminosity. For comparison, a classic steady accretion disk component between r_{in} and r_{out} , the gap region, is shown as a blue dotted curve. The black dotted line is the classic $\epsilon^{1/3}$ spectrum.

on the radial scale of the gap, and our best estimate of turbulent dissipation within the streams is that it should be $< 1\%$ of the shock heating, it seems unlikely that their luminosity can be more than a rather small fraction of the ordinary accretion luminosity produced either near the inner edge of the circumbinary disk or near the outer edges of the mini-disks around the members of the binary. For this reason, we disagree with the claim made by [Farris et al. \(2015\)](#), who applied an “ α -viscosity” model to stream fluid dynamics, that the streams should, if anything, be brighter than the adjacent portions of the disks. Instead, our results support the prediction of [Roedig et al. \(2014\)](#) that the thermal continua of accreting binaries should be marked by a “notch” centered on the frequencies corresponding to the temperature an ordinary disk would have on a radial scale of order the binary separation.

For typical parameters of supermassive binary black holes, the characteristic disk temperature

scales as

$$T_0 = 1.9 \times 10^4 \left(\frac{\eta}{0.1}\right)^{-1/4} \left(\frac{\dot{M}}{\dot{M}_E}\right)^{1/4} \times \left(\frac{M}{10^8 M_\odot}\right)^{-1/4} \left(\frac{a}{10^2 R_g}\right)^{-3/4} \text{ K}, \quad (9)$$

where $\dot{M}_E \equiv L_E/(\eta c^2)$, with η denoting the accretion energy conversion rate, R_g the Schwarzschild radius, \dot{M} the outer disk accretion rate, and L_E the Eddington luminosity. The typical energy scale shown in Figure 7 is then $\sim 0.1\text{--}10\text{ eV}$ if the binary separation is $\sim 100R_g$, $\eta \sim 0.1$, and \dot{M} and M are not too far from \dot{M}_E and $10^8 M_\odot$ respectively.

We can also estimate the typical optical depth in the gas streams based on their surface density in our simulations. In code units, we find this varies within the range $\sim 0.1\text{--}0.5\Sigma_0$. If we assume that electron scattering opacity dominates, the implied optical depth is

$$\tau_T \simeq (92\text{--}460) \left(\frac{\eta}{0.1}\right)^{-1} \left(\frac{\dot{M}}{\dot{M}_E}\right) \left(\frac{a}{10^2 R_g}\right)^{-1/2}. \quad (10)$$

Thus, for $\eta \sim 0.1$ and $\dot{M} \lesssim \dot{M}_E$, we expect Thomson optical depths $\tau_T \sim 100$ when the binary sep-

aration is about $100R_g$. Adopting Kramer’s law for absorption opacity, we have

$$\begin{aligned}\tau_a &= 3.2 \times 10^{22} \Sigma^2 H^{-1} T_{\text{eff}}^{-7/2} \quad (11) \\ &\simeq (2.5-65) \times 10^{-4} \left(\frac{\eta}{0.1}\right)^{-9/8} \left(\frac{\dot{M}}{\dot{M}_E}\right)^{9/8} \\ &\times \left(\frac{M}{10^8 M_\odot}\right)^{-15/8} \left(\frac{a}{10^2 R_g}\right)^{13/8}.\end{aligned}$$

Here we adopt $\Sigma = 2\rho H$ and $H \equiv c_s/\Omega(r) = 0.1(r/a)^{3/2} a$ with $r = 1.5a$ for the location of the stream. To obtain this number, we estimated the effective temperature using Equation 7; it is a factor of a few greater than T_0 . Together with τ_T , we find the effective absorption optical depth is

$$\begin{aligned}\tau_* &\simeq \sqrt{\tau_T \tau_a} \quad (12) \\ &\simeq (0.15 - 1.73) \left(\frac{\eta}{0.1}\right)^{-17/16} \left(\frac{\dot{M}}{\dot{M}_E}\right)^{17/16} \\ &\times \left(\frac{M}{10^8 M_\odot}\right)^{-15/16} \left(\frac{a}{10^2 R_g}\right)^{9/16}.\end{aligned}$$

Again taking $\eta \sim 0.1$ and \dot{M} close to \dot{M}_E , we find the effective opacity is roughly order unity. However, the scale height of our simulation ($H/R \sim 0.1$) is likely an overestimate of the scale height in a realistic disk in these circumstances, so that the absorption optical depth, which is $\propto H^{-1/2}$, might be rather larger. If so, the spectrum radiated even by the streams would be reasonably well thermalized.

The temperature at the stream surface should closely track the shock heating rate in the interior of the stream because the cooling time should be at worst comparable to the disk dynamical time, and likely shorter. Even using the simulation scale height, we find:

$$\begin{aligned}t_{\text{cool}}\Omega &\simeq H\Omega\tau/c \quad (13) \\ &\simeq (0.64-0.33) \left(\frac{\eta}{0.1}\right)^{-1} \left(\frac{\dot{M}}{\dot{M}_E}\right) \left(\frac{a}{10^2 R_g}\right)^{-1}.\end{aligned}$$

In fact, the short cooling time gives some justification to our assumption of an isothermal equation of state in treating the shocks.

We close this discussion with one last remark. In ordinary accretion disks, matter traversing a

factor of several in radius must lose significant energy to do so; that raises the question of what happens to the energy the streams don’t radiate. The answer is that when these shocks join the binary, they do so by striking the outer edge of one of the mini-disks surrounding each black hole. As [Roedig et al. \(2014\)](#) showed, there is a very strong shock where this happens, in which the Compton cooling time is very short. Thus, the energy not lost by slow thermal emission is instead lost rapidly by Compton cooling at the edge of a mini-disk. In a fashion attractive to observations, it would also be modulated with a frequency of order that of the binary. However, it plays no role in the thermal spectrum because the characteristic energy of the Compton-scattered photons is ~ 100 keV.

JS was supported in part by the National Science Foundation under grant PHY-1144374, ”A Max-Planck/Princeton Research Center for Plasma Physics” and grant PHY-0821899, ”Center for Magnetic Self-Organization”. JHK also acknowledges support from the NSF, but through grant AST-1516299.

REFERENCES

- Andrews, S. M. & Williams, J. P. 2005, *ApJ*, 631, 1134
- Artymowicz, P. & Lubow, S. H. 1994, *ApJ*, 421, 651
- Balbus, S. A. & Hawley, J. F. 1998, *Reviews of Modern Physics*, 70, 1
- Begelman, M. C., Blandford, R. D., & Rees, M. J. 1980, *Nature*, 287, 307
- Billar, B. A., Males, J., Rodigas, T., Morzinski, K., Close, L. M., Juhász, A., Follette, K. B., Lacour, S., Benisty, M., Sicilia-Aguilar, A., Hinz, P. M., Weinberger, A., Henning, T., Pott, J.-U., Bonnefoy, M., & Köhler, R. 2014, *ApJ*, 792, L22
- Cuadra, J., Armitage, P. J., Alexander, R. D., & Begelman, M. C. 2009, *MNRAS*, 393, 1423
- de Val-Borro, M., Gahm, G. F., Stempels, H. C., & Pepliński, A. 2011, *MNRAS*, 413, 2679
- D’Orazio, D. J., Haiman, Z., Duffell, P., MacFadyen, A., & Farris, B. 2016, *MNRAS*, 459, 2379

- D’Orazio, D. J., Haiman, Z., & MacFadyen, A. 2013, *MNRAS*, 436, 2997
- Dutrey, A., Guilloteau, S., & Simon, M. 1994, *A&A*, 286
- Farris, B. D., Duffell, P., MacFadyen, A. I., & Haiman, Z. 2014, *ApJ*, 783, 134
- . 2015, *MNRAS*, 447, L80
- Gültekin, K. & Miller, J. M. 2012, *ApJ*, 761, 90
- Günther, R. & Kley, W. 2002, *A&A*, 387, 550
- Hanawa, T., Ochi, Y., & Ando, K. 2010, *ApJ*, 708, 485
- Ivanov, P. B., Papaloizou, J. C. B., & Polnarev, A. G. 1999, *MNRAS*, 307, 79
- Kocsis, B., Haiman, Z., & Loeb, A. 2012, *MNRAS*, 427, 2660
- MacFadyen, A. I. & Milosavljević, M. 2008, *ApJ*, 672, 83
- Merritt, D. & Milosavljević, M. 2005, *Living Reviews in Relativity*, 8
- Noble, S. C., Mundim, B. C., Nakano, H., Krolik, J. H., Campanelli, M., Zlochower, Y., & Yunes, N. 2012, *ApJ*, 755, 51
- Reggiani, M., Quanz, S. P., Meyer, M. R., Pueyo, L., Absil, O., Amara, A., Anglada, G., Avenhaus, H., Girard, J. H., Carrasco Gonzalez, C., Graham, J., Mawet, D., Meru, F., Milli, J., Osorio, M., Wolff, S., & Torrelles, J.-M. 2014, *ApJ*, 792, L23
- Roedig, C., Krolik, J. H., & Miller, M. C. 2014, *ApJ*, 785, 115
- Roedig, C. & Sesana, A. 2012, *Journal of Physics Conference Series*, 363, 012035
- Roedig, C., Sesana, A., Dotti, M., Cuadra, J., Amaro-Seoane, P., & Haardt, F. 2012, *A&A*, 545, A127
- Sallum, S., Follette, K. B., Eisner, J. A., Close, L. M., Hinz, P., Kratter, K., Males, J., Skemer, A., Macintosh, B., Tuthill, P., Bailey, V., Defrère, D., Morzinski, K., Rodigas, T., Spalding, E., Vaz, A., & Weinberger, A. J. 2015, *Nature*, 527, 342
- Shakura, N. I. & Sunyaev, R. A. 1973, *A&A*, 24, 337
- Shi, J.-M. & Krolik, J. H. 2015, *ApJ*, 807, 131
- Shi, J.-M., Krolik, J. H., Lubow, S. H., & Hawley, J. F. 2012, *ApJ*, 749, 118
- Stone, J. M. & Norman, M. L. 1992, *ApJS*, 80, 753
- Tanaka, T., Menou, K., & Haiman, Z. 2012, *MNRAS*, 420, 705
- Tanaka, T. L. & Haiman, Z. 2013, *Classical and Quantum Gravity*, 30, 224012